Original Articles

Manufacturing Method and Build Orientation Influence Alkali-Heat Treated Titanium (Ti-6Al-4V) Dental Implant Surface Characteristics

Tuan Hoang Nguyen [1], Phetcharat Dhammayannarangsi[2], Viritpon Srimaneepong[3], Patcharapit Promoppatum[4], Chalida Nakalekha Limjeerajarus[5,6], Nuttapol Limjeerajarus[7]

[1]Graduate Program in Oral Biology, Faculty of Dentistry, Chulalongkorn University, Bangkok, Thailand
[2]Department of Dental Biomaterials Science, Graduate School, Faculty of Dentistry, Chulalongkorn University, Bangkok, Thailand
[3]Department of Prosthodontics, Faculty of Dentistry, Chulalongkorn University, Bangkok, Thailand
[4]Center for Lightweight Materials, Design, and Manufacturing, Department of Mechanical Engineering, Faculty of Engineering, King Mongkut's University of Technology Thonburi (KMUTT), Bangkok, Thailand
[5]Center of Excellence for Dental Stem Cell Biology, Faculty of Dentistry, Chulalongkorn University, Bangkok, Thailand
[6]Department of Physiology, Faculty of Dentistry, Chulalongkorn University, Bangkok, Thailand
[7]Office of Academic Affairs, Faculty of Dentistry, Chulalongkorn University, Bangkok, Thailand

Abstract

This study examined the impact of alkali-heat treatment on the surface properties of Ti-6Al-4V titanium implants fabricated by conventional machining and laser powder bed fusion (LPBF) additive manufacturing with horizontal and vertical build orientations. Disc-shaped specimens were produced, immersed in 10 M NaOH at 90 °C for 24 hours, and heat-treated at 600 °C. Scanning electron microscopy revealed uniform nanostructures, such as nanospikes and crevices, across all treated groups while preserving the original microtopography. Energy-dispersive X-ray spectroscopy and X-ray diffraction confirmed the formation of a sodium titanate layer, indicated by increased sodium and oxygen content and a new diffraction peak at 48.3°. Surface roughness analysis showed that LPBF samples had significantly higher roughness than machined ones ($p < 0.0001$), with horizontally printed specimens rougher than vertically printed counterparts ($p < 0.05$). Importantly, the treatment did not significantly alter the initial roughness in any group ($p > 0.1$). These findings demonstrate that alkali-heat treatment effectively creates bioactive nanostructures and modifies the surface chemistry of titanium implants without compromising their roughness or microtopography. Moreover, build orientation influences surface characteristics, highlighting the importance of optimizing manufacturing parameters. Overall, combining LPBF fabrication with alkali-heat treatment may enhance the bioactivity of complex titanium implants for dental applications.

Keywords: Alkali-heat treatment, Dental implants, Laser powder bed fusion (LPBF), Surface modification, Ti-6Al-4V

Received date: Jul 7, 2025 **Revised date:** Sep 5, 2025 **Accepted date:** Sep 15, 2025

Doi: 10.14456/jdat.2025.26

Correspondence to:
Nuttapol Limjeerajarus, Office of Academic Affairs, Faculty of Dentistry, Chulalongkorn University, Henri Dunant Rd., Bangkok, 10330, Thailand. Email: Nuttapol.l@chula.ac.th

article in press

Introduction

Dental implants have become the standard treatment for replacing missing teeth, with titanium implants widely used due to their excellent biocompatibility and mechanical properties, enabling effective osseointegration with bone.[1,2]

However, titanium and its alloys, particularly Ti-6Al-4V, are inherently bioinert, which can limit direct bone bonding.[3] The physico-chemical properties of biomaterials used for fabricating implants, including surface microtopography, chemical composition, and wettability, significantly influence the host cellular activity, which in turn affects treatment outcomes.[4] Hence to enhance the bioactivity of implant surfaces, a variety of surface modification techniques have been developed, such as alkali-heat treatment, sandblasting, acid etching, anodization, and plasma spraying.[5,6]

Of these, surface modification using sodium hydroxide (NaOH) has been shown to improve the bioactivity of titanium implants, due to the formation of a highly bioactive sodium titanate layer.[7] In particular, this layer enhances hydrophilicity, roughness, and cell compatibility of the implant surface.[4,8] The outcomes of such alkali treatment with sodium hydroxide (NaOH) depend on several factors, including the concentration and temperature, treatment duration, and the initial surface microtopography.[8,9] Studies on conventionally machined titanium implants have demonstrated that alkali-heat treatment can influence the behavior of host cell types, including macrophages, gingival fibroblasts, osteocytes, and periodontal ligament cells, prompting them to exhibit functions suited to their surroundings.[8,10-15]

Moreover, different implant production methods result in varying mechanical and physical properties.[16,17] While most titanium implants have been produced using subtractive manufacturing, additive manufacturing (AM), particularly laser powder bed fusion (LPBF), has recently gained attention for fabricating patient-specific titanium implants with optimal mechanical strength and biocompatibility.[18,19] This technique, also called three-dimensional (3D) printing, is a computer-controlled process that translates 3D structural information into parts by melting materials layer by layer.[20] The LPBF method allows precise control over several manufacturing parameters impacting implant properties, such as the laser power, scanning speed, scanning pattern, powder layer thickness, and building orientation.[21,22] Additionally, the building orientation in LPBF can influence the physical and mechanical properties of the implant, including surface roughness, wettability, and free energy, all of which can modulate cell responses.[16,23,24] In addition to enhancing bioactivity, surface modification techniques such as chemical and electrochemical methods have been applied to 3D-printed titanium implants to remove the unmelted particles, particularly in porous scaffolds.[25] However, there have been no previous studies comparing alkali-heat treatment effects across machining and LPBF orientations.

Hence in the present study, two different production methods, additive, laser powder bed fusion (LPBF) and subtractive manufacturing to treat Ti-6Al-4V discs were evaluated. The LPBF specimens were printed in two different building directions: horizontal (0°) and vertical (90°). Half of the samples from each group underwent alkali-heat treatment, which involved immersion in a 10 M NaOH solution at 90°C for 24 hours, followed by heat treatment at 600°C for 1 hour. The remainder of the sample was used as negative controls.

The current study aims to evaluate the effects of alkali-heat treatment on surface topography, physical properties, and chemical composition of additively manufactured titanium implants with different building orientations. We therefore hypothesized that such treatment and manufacturing parameters would significantly alter the properties of the materials, providing valuable insights into the relationship between production methods and surface modification outcomes.

Materials and methods

Sample Size Calculations

For surface characterization, three samples per group were analyzed by the Scanning Electron Microscopy (SEM) and the Energy Dispersive X-ray Spectroscopy (EDS), while one sample per group was used for X-ray Diffraction (XRD). The sample size for roughness analysis was determined using G*Power with a significance level of 0.05, a power of 0.80, and an effect size of 2.11 from prior research[16], yielding a calculated minimum of two samples. To allow for a 10% margin of error, three specimens per experimental group were included for roughness measurements.

Preparation of Titanium Specimens

The disc-shaped titanium samples (10 mm diameter, 2 mm thickness) were fabricated via machining and laser powder bed fusion (LPBF). LPBF specimens were built in

horizontal (0°) and vertical (90°) orientations. A 3D model created in ANSYS Spaceclaim was prepared in Materialise Magics Print and printed from Ti-6Al-4V ELI powder (15–45 µm; AP&C, Canada) using a TruPrint 1000 machine (Trumpf, Germany). Process parameters included 100 W laser power, 1200 mm/s scanning speed, 80 µm hatch spacing, 20 µm layer thickness, and 30 µm laser spot diameter in an argon atmosphere (≤100 ppm oxygen). Printed specimens were removed by wire-cut EDM. Machined specimens were cut from Ti-6Al-4V ELI rods and sequentially polished with 400–1200 grit silicon carbide paper. All samples were ultrasonically cleaned with deionized water, acetone, ethanol, and DI water.

Surface modification involved immersion in 10 M NaOH at 90 °C for 24 hours, rinsing, air drying, and sintering at 600 °C for 1 hour.[10-12] Six experimental groups were prepared: non-treated machined (M), non-treated horizontally printed (H), non-treated vertically printed (V), treated machined (TM), treated horizontally printed (TH), and treated vertically printed (TV) specimens.

Scanning Electron Microscope and Energy Dispersive X-ray Spectroscopy

The surface topography and chemical composition of the six groups of titanium samples were evaluated using a scanning electron microscope (SEM) equipped with an energy-dispersive X-ray spectroscopy (EDS) (Quanta 250, FEI, USA). Prior to analysis, the prepared samples were stored in a desiccator overnight. SEM and EDS analyses were performed in high vacuum mode with an acceleration voltage of 20 kV. For SEM imaging, magnifications of 1,000×, 10,000×, and 50,000× were used to observe surface features. The SEM working distance ranged from 7.7 to 10 mm, and the spot size was set to 3.0. EDS analysis was conducted to determine the weight percentages (wt%) of elements present on the specimen surfaces at 1,000× magnification. The EDS working distance and spot size were set to 10 mm and 5.6, respectively.

X-ray Diffraction Analysis

X-ray diffraction (XRD) was conducted to identify the chemical composition and crystal structure of titanium samples produced by two different methods, with and without alkali-heat treatment. The analysis was performed at room temperature using a diffractometer (D8 Discover, Bruker, Germany) with Cu Kα radiation. Data was continuously collected over a 2θ range of 10° to 80° at a scan rate of 0.02° per second. The resulting diffraction data was analyzed using OriginPro (version 2025, OriginLab Corporation, Northampton, MA, USA).

Roughness Analysis

Surface roughness parameters, such as the arithmetic mean height (Ra), average roughness over an area (Sa), and 3D roughness profile were evaluated for six groups of titanium specimens. Each group consisted of three samples, and three locations were measured per sample. The assessments were conducted with 10x lens using an optical profilometer (Alicona InfiniteFocus SL, Austria). Scanning was performed using the ALICONA Laboratory Measurement Module 5.4, and the results were analyzed with ALICONA MeasureSuite software (Alicona, Austria).

Data Analysis

The weight percentages (wt%) of elements obtained from EDS analysis and surface roughness data (Sa and Ra) from the six experimental groups were analyzed. Normality was confirmed using the Shapiro-Wilk test. Since the data were normally distributed, a one-way ANOVA was performed to compare the six groups, followed by Tukey's post hoc test for pairwise comparisons. All data were reported as mean±SD. Statistical significance was set at $p < 0.05$. Data analysis was performed using GraphPad Prism (version 10.3.1, GraphPad Software, Boston, USA).

Results

Surface Topography of Differently Produced and Modified Titanium Specimens

The surface topography of titanium specimens, produced by different methods and modified via alkali-heat treatment, was examined using a scanning electron microscopy (SEM). In both vertically and horizontally printed LPBF samples, spherical particles were observed (Fig. 1C1, E1), with the vertically printed specimens showing a denser particle distribution. In contrast, the machined samples (Fig. 1A1) exhibited relatively smooth surfaces marked by polishing-induced scratches. At higher magnifications (10,000× and 50,000×), the unmodified specimens (Fig. 1A2, C2, E2, A3, C3, E3) displayed relatively smooth surfaces. After alkali-heat treatment, all modified groups at 1,000× (Fig.

1B1, D1, F1) showed uneven surface deposition while still retaining visible features of the original microtopography. At 10,000× magnification (Fig. 1B2, D2, F2), irregularly distributed cracks and nanocrevices were observed. At 50,000x (Fig. 1B3, D3, F3), the modified surfaces revealed numerous nanospikes with a porous surface texture.

Surface Chemistry of Differently Produced and Modified Titanium Specimens

Energy-dispersive X-ray spectroscopy (EDS) characterized the titanium surfaces quantitatively (Table 1). Within both the non-treated and treated groups, most elements did not differ significantly between manufacturing methods. Untreated machined, horizontally, and vertically printed samples contained over 80 wt% titanium, with minor aluminum, vanadium, oxygen, and carbon evenly distributed. However, the aluminum and oxygen levels in the untreated vertical specimens were significantly different from those in the other two untreated groups. The analysis revealed statistically significant differences in chemical composition between treated and untreated groups, except for the proportion of carbon. Specifically, alkali-heat treatment significantly reduced titanium content to 46–48 wt%, increased oxygen to 39–42 wt%, and introduced sodium (5.12–5.82 wt%), suggesting sodium titanate formation. In the treated groups, the vertically printed samples exhibited the highest oxygen content, while the machined samples had the lowest. These results demonstrate that alkali-heat treatment alters surface chemistry by decreasing the proportion of metallic elements and enriching oxygen and sodium.

X-ray diffraction (XRD) was employed to further examine the chemical composition and crystalline structure of the titanium samples (Fig. 2). All groups exhibited strong diffraction peaks corresponding to the hexagonal close-packed (α-phase) titanium (PDF 04-004-9156), with prominent peaks near 35.5°, 38.6°, 40.5°, 53.4°, and 63.6°. A weaker peak around 39.5°, associated with the body-centered cubic (β-phase) titanium (PDF 04-019-6427), was observed in both machined and treated machined specimens, indicating the presence of α–β titanium alloys. Following alkali-heat treatment, a new low-intensity diffraction peak emerged in all treated groups, notably at 48.3°, which did not correspond to either the α- or β-Ti phases.

Surface Roughness of Differently Produced and Modified Titanium Specimens

Three-dimensional surface profiles (Fig. 3A–F), obtained using an optical profilometer, qualitatively illustrate the topography of the specimens. These profiles were further evaluated to determine surface roughness parameters, including arithmetic mean height (Ra) and area roughness (Sa). Quantitative roughness analysis is shown in Fig. 3G, H. Machined and treated machined surfaces exhibited the lowest Ra and Sa values, indicating smoother topographies. In contrast, horizontally and vertically printed surfaces showed significantly higher roughness, with horizontally printed samples exhibiting the highest Ra and Sa values, followed by vertically printed ones. Notably, alkali-heat treatment did not significantly alter the surface roughness across any of the groups.

Table 1 *Chemical Composition of Different Titanium Surfaces*

Treatment	Groups	Element (wt%) (Mean±SD)					
		Titanium (Ti)	Aluminum (Al)	Vanadium (V)	Oxygen (O)	Carbon (C)	Sodium (Na)
Untreated	M	81.35±0.16^{A}	5.50±0.09^{A}	3.05±0.08^{A}	6.03±0.38^{A}	4.07±0.22^{AB}	0±0^{A}
	H	81.26±0.84^{A}	5.69±0.25^{A}	2.96±0.12^{A}	6.03±0.40^{A}	4.06±0.55^{AB}	0±0^{A}
	V	80.83±0.38^{A}	4.80±0.03^{B}	3.20±0.07^{A}	7.59±0.28^{B}	3.58±0.06^{B}	0±0^{A}
Treated	TM	48.45±1.53^{B}	1.06±0.28^{C}	1.06±0.17^{B}	39.31±0.79^{C}	5.00±0.62^{A}	5.12±0.62^{B}
	TH	46.79±2.02^{B}	0.68±0.13^{C}	0.86±0.06^{B}	40.73±0.75^{CD}	5.13±0.61^{A}	5.82±0.85^{B}
	TV	46.30±0.61^{B}	0.70±0.06^{C}	0.86±0.02^{B}	41.72±0.17^{D}	5.03±0.26^{A}	5.40±0.28^{B}

Legend. *M (Machined); H (Horizontally Printed); V (Vertically Printed); TM (Treated Machined); TH (Treated Horizontally Printed); TV (Treated Vertically Printed). Different superscript capital letters within the same column indicate significant differences between the six titanium surfaces (one-way ANOVA with Tukey's post hoc test, $p < 0.05$).*

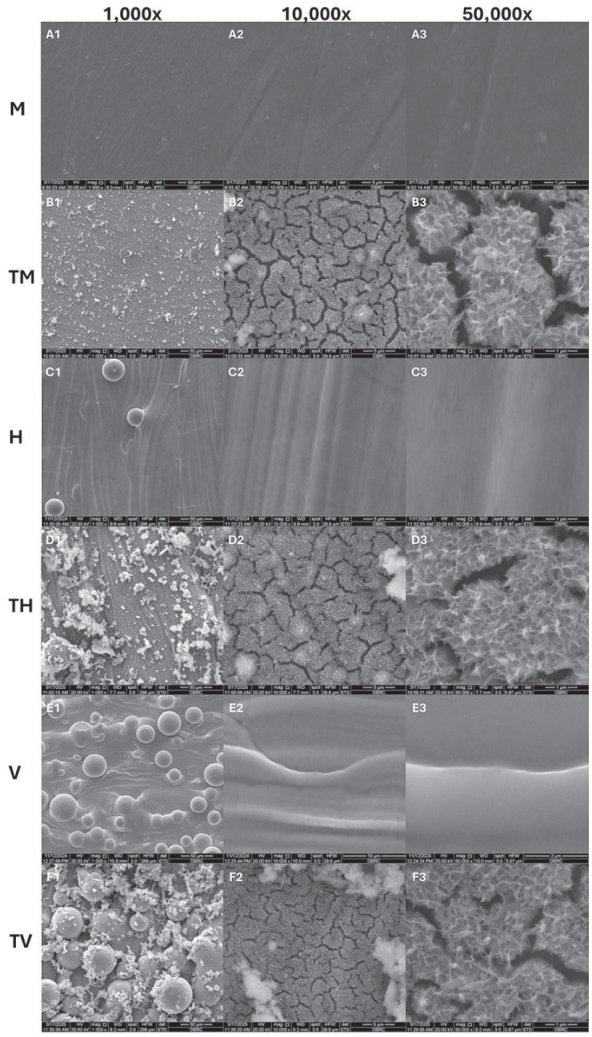

Figure 1 *Scanning Electron Micrographs of Different Titanium Surfaces at 1,000×, 10,000×, and 50,000× Magnifications (A1–A3) Untreated machined (M) specimens show smooth surfaces with polishing marks. (C1–C3) Horizontally printed (H) specimens exhibit globular particles with uniform distribution. (E1–E3) Vertically printed (V) specimens show denser particle accumulation. (B1, D1, F1) Alkali-heat-treated surfaces (TM, TH, TV) display surface deposits while retaining microtopography. (B2, D2, F2) At 10,000×, scattered cracks and nanoscale crevices are visible. (B3, D3, F3) At 50,000×, nanospikes and porous morphology appear.*

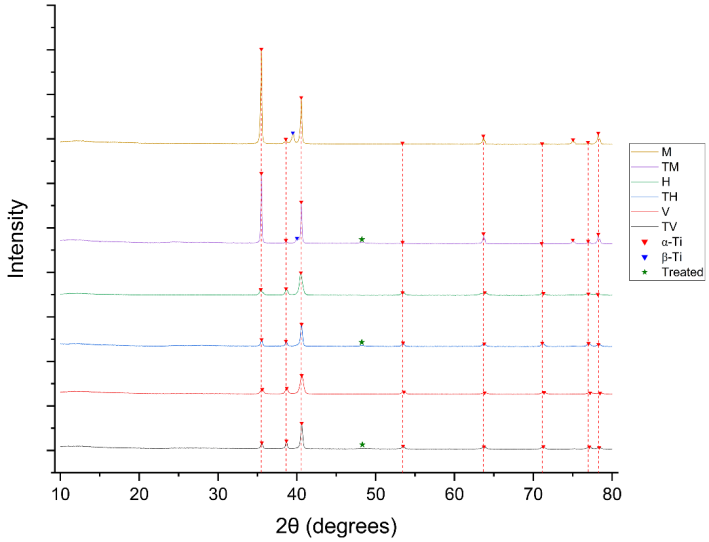

Figure 2 *XRD Patterns of Different Titanium Surfaces*
M, Machined; TM, Treated Machined; H, Horizontally Printed; TH, Treated Horizontally Printed; V, Vertically Printed; TV, Treated Vertically Printed.
Red Triangle: Peaks corresponding to α-phase titanium; Blue Triangle: Peaks corresponding to β -phase

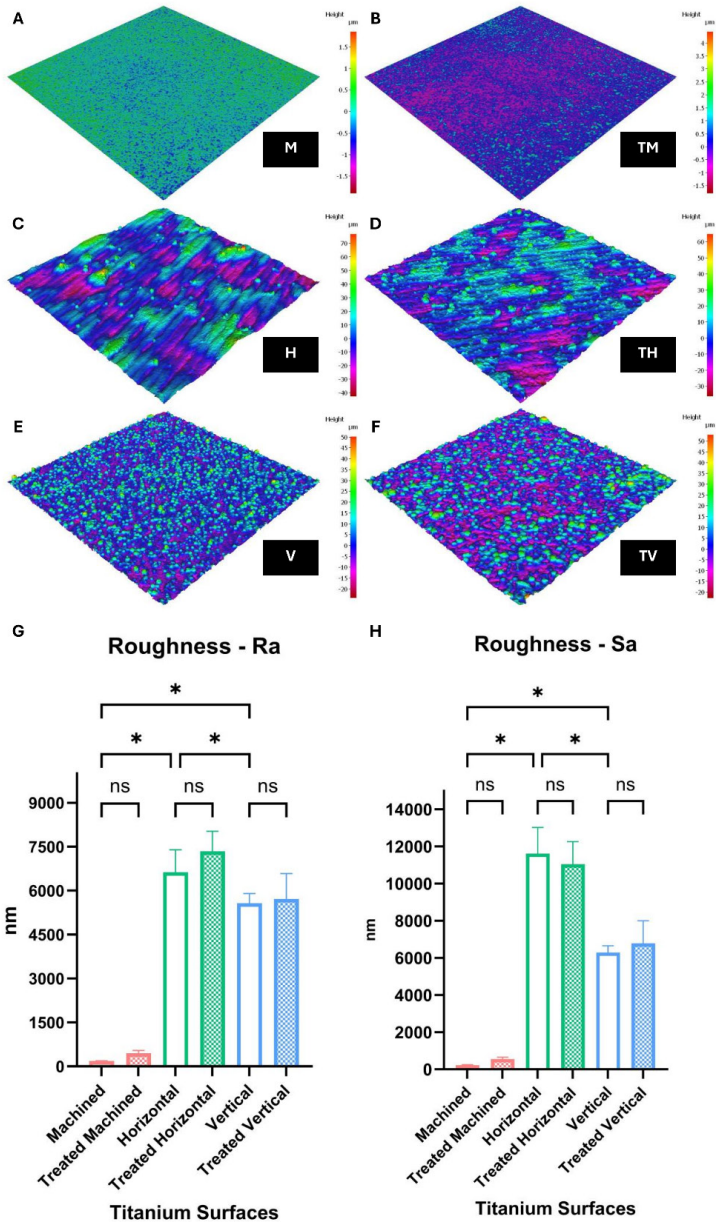

Figure 3 3D Roughness Profile and Roughness Parameters Analysis
(A-F) *3D Roughness Profiles of different titanium surfaces*
M, Machined; TM, Treated Machined; H, Horizontally Printed; TH, Treated Horizontally Printed; V, Vertically Printed; TV, Treated Vertically Printed. (G) Mean arithmetic mean height (Ra); (H) Mean area roughness (Sa) of different titanium surfaces. Data are presented as means±standard deviation (SD). The asterisks indicate the statistical significance ($p < 0.05$; Tukey's honest significant difference [HSD] test).

Discussion

This study aimed to assess how alkali-heat treatment affects the surface characteristics of Ti-6Al-4V specimens produced by different manufacturing methods including subtractive (machined) and additive (LPBF with horizontal and vertical orientations). The findings show that both the production method and the surface modification technique significantly influence surface morphology, chemistry, and roughness of the titanium implant.

SEM imaging revealed clear distinctions in surface topography between production methods. As expected, machined specimens exhibited smooth surfaces with polishing marks, while LPBF-produced specimens showed prominent spherical particles, more densely distributed in vertically printed samples. The presence and distribution of partially melted powder remnants described in the present study are commonly observed

in LPBF-manufactured titanium surfaces with different building directions.[16,17] Following alkali-heat treatment, all groups displayed significant morphological changes, including nanospikes and nanocrevices distributed unevenly across the surface, which align with previous observations of sodium titanate nanostructure formation.[8,11] Furthermore, the nanotopography created by alkali-heat treatment has been shown to influence osseointegration. Previous studies using the same treatment on machined samples have shown that the resulting titanium surfaces can promote the formation of an osteocyte lacunar–canalicular network and enhance peri-implant osseointegration.[10,14] In this study, SEM images revealed similar nanostructures on both machined and LPBF specimens, suggesting comparable properties. However, further *in vitro* and *in vivo* investigations are needed to confirm these findings. Interestingly, the LPBF-manufactured samples retained much of their original microtopography after alkali-heat treatment, while the machined surfaces became noticeably more textured. This suggests that the treatment has a more pronounced effect on the nanotopography of titanium surfaces.

EDS analysis confirmed a substantial shift in surface composition after alkali-heat treatment. Untreated specimens consisted primarily of titanium, aluminum, and vanadium, consistent with Ti-6Al-4V alloy composition. Notably, a high proportion of carbon was detected across all groups, likely indicating surface contamination from handling, the environment, or the sample preparation process, which has also been reported in a previous titanium surface study.[26] Since the contamination was present across all groups at comparable levels, it should not affect the relative comparisons or overall interpretations of elemental changes after alkali-heat treatment. Post-treatment, there was a marked increase in oxygen and the appearance of sodium, indicating successful formation of a sodium titanate layer, a key objective of this study. These results are consistent with earlier studies reporting the transformation of titanium surfaces through NaOH treatment into bioactive titanate layers.[7,11,27] The higher oxygen content after alkali-heat treatment reflects the formation of a thicker TiO_2 layer that could increase surface wettability and facilitate osteoblast attachment.[28] The sodium detected on the surface originates from sodium titanate, which can undergo ion exchange with protons under physiological conditions, generating Ti-OH groups that promote apatite nucleation.[7,29] This bioactive apatite layer has been shown to mediate strong bone bonding, consistent with prior *in vitro* and *in vivo* studies demonstrating improved osseointegration of alkali heat–treated titanium implants.[10,12,30,31]

XRD analysis further supported the observed compositional changes. Untreated samples exhibited dominant peaks corresponding to the α-Ti phase, with minor β-phase peaks, consistent with previous studies.[16,32] In Ti-6Al-4V, the α-phase provides strength and corrosion resistance, while the β-phase contributes ductility.[33] In this study, β-phase peaks were observed only in the machined specimens, while LPBF-produced samples exhibited predominantly α-phase, could be due to the rapid cooling suppressing β-phase retention.[34] Since these phases mainly influence the mechanical properties of the alloy, their distribution may affect implant stability, whereas biological performance is more directly related to surface chemistry and topography. Following alkali-heat treatment, all groups displayed a new diffraction peak around 48.3°, likely associated with the formation of sodium titanate. The presence of this peak across all treated groups, regardless of manufacturing method, indicates that the alkali-heat process reliably induces a chemical phase transformation. However, the relatively low intensity and the appearance of only a single sodium titanate peak suggest that further investigation is necessary to confirm the extent and crystallinity of the newly formed phase.

Surface roughness analysis revealed that LPBF specimens, particularly those printed in the horizontal orientation, had significantly higher Ra and Sa values than machined specimens, both before and after treatment. This aligns with prior findings where LPBF processes inherently produce rougher surfaces due to powder sintering characteristics and layer-by-layer fabrication.[16,24,35] However, some studies have reported that vertically printed specimens typically demonstrate greater surface roughness than those printed horizontally, which contrasts with the findings of the present study.[16,32] This discrepancy may be explained by differences in measurement instruments and magnifications. Our analysis was performed using an optical profilometer with a 10×

lens and a scan area of 2 × 2 mm. In contrast, Celles *et al* used a laser confocal microscope at 428× magnification and reported vertically printed samples to be rougher.[16] Similarly, Huang *et al.* employed both a contact profilometer and atomic force microscopy (scan areas of 500 µm × 500 µm and 5 µm × 5 µm, respectively) and found higher roughness in vertical specimens.[26] To the best of our knowledge, our study is the first to report horizontal orientation producing a rougher surface. This may be due to larger scan areas capturing greater disparities between peaks and valleys, or to limitations of the measurement technique, in which densely packed particles could prevent full detection of the deepest points on the surface.

Contrary to some expectations based on previous literature[8,12], alkali-heat treatment did not significantly alter the surface roughness in any of the experimental groups. This may be attributed to the already high baseline roughness of the LPBF specimens, which could have masked subtle changes, or to limitations in the resolution of the measurement equipment, which may not effectively capture nanoscale modifications.

A key limitation of this study is its exclusive focus on the chemical composition and physical surface properties of titanium implants. While these characteristics provide valuable insights into material performance, they do not capture the biological interactions critical to clinical outcomes. Therefore, future research should include both *in vitro* and *in vivo* studies to evaluate cellular responses and determine the clinical relevance of the different production methods and surface treatments.

Conclusion

This study shows that both the manufacturing method and alkali-heat treatment influence the surface properties of Ti-6Al-4V implants. While the elemental composition remained consistent, the manufacturing method led to distinct differences in surface topography. Machined specimens exhibited an α–β phase, whereas LPBF specimens showed an α phase. Surface roughness was also higher in LPBF implants compared with machined ones, with horizontal LPBF rougher than vertical. Alkali-heat treatment effectively modified the surface chemistry by forming a sodium titanate layer without significantly changing roughness. Overall, these findings indicate that optimizing processing and surface modification can tailor surface properties to potentially enhance bioactivity, although further biological validation is needed.

Acknowledgement

This project was supported by the National Research Council of Thailand and the Faculty of Dentistry Chulalongkorn Dental Research Grant. The authors gratefully acknowledge Assist. Prof. Dr. Soranun Chantarangsu for reviewing the statistical analysis methodology, and K Dental Laboratory for providing the furnace used in the heat treatment process.

References

1. Gupta R, Gupta N, Weber DK. Dental Implants. StatPearls. Treasure Island (FL)2024.

2. Zhang K, Zhang B, Huang C, Gao S, Li B, Cao R, *et al.* Biocompatibility and antibacterial properties of pure titanium surfaces coated with yttrium-doped hydroxyapatite. ***J Mech Behav Biomed Mater*** 2019; 100:103363.

3. Van Noort R. Titanium: the implant material of today. ***J Mater Sci*** 1987;22:3801-11.

4. Feller L, Jadwat Y, Khammissa RA, Meyerov R, Schechter I, Lemmer J. Cellular responses evoked by different surface characteristics of intraosseous titanium implants. ***Biomed Res Int*** 2015;2015:171945.

5. Inchingolo AM, Malcangi G, Ferrante L, Del Vecchio G, Viapiano F, Inchingolo AD, *et al.* Surface Coatings of Dental Implants: A Review. ***J Funct Biomater*** 2023;14(5):287.

6. Mandracci P, Mussano F, Rivolo P, Carossa S. Surface treatments and functional coatings for biocompatibility improvement and bacterial adhesion reduction in dental implantology. ***Coatings*** 2016;6(1):7.

7. Kokubo T, Yamaguchi S. Bioactive titanate layers formed on titanium and its alloys by simple chemical and heat treatments. ***Open Biomed Eng J*** 2015;9:29-41.

8. Kato E, Sakurai K, Yamada M. Periodontal-like gingival connective tissue attachment on titanium surface with nano-ordered spikes and pores created by alkali-heat treatment. ***Dent Mater*** 2015;31 (5):e116-30.

9. Pattanayak DK, Fukuda A, Matsushita T, Takemoto M, Fujibayashi S, Sasaki K, *et al.* Bioactive Ti metal analogous to human cancellous bone: Fabrication by selective laser melting and chemical treatments. ***Acta Biomater*** 2011;7(3):1398-406.

10. He X, Yamada M, Watanabe J, Pengyu Q, Chen J, Egusa H. Titanium nanotopography enhances mechano-response of osteocyte three-dimensional network toward osteoblast activation. ***Biomater Adv*** 2024;163:213939.

11. Yamada M, Kimura T, Nakamura N, Watanabe J, Kartikasari N, He X, *et al.* Titanium Nanosurface with a Biomimetic Physical

Microenvironment to Induce Endogenous Regeneration of the Periodontium. ***ACS Appl Mater Interfaces*** 2022;14(24):27703-19.
12. Kartikasari N, Yamada M, Watanabe J, Tiskratok W, He X, Kamano Y, *et al.* Titanium surface with nanospikes tunes macrophage polarization to produce inhibitory factors for osteoclastogenesis through nanotopographic cues. ***Acta Biomater*** 2022;137:316-30.
13. Kartikasari N, Yamada M, Watanabe J, Tiskratok W, He X, Egusa H. Titania nanospikes activate macrophage phagocytosis by ligand-independent contact stimulation. ***Sci Rep*** 2022;12(1):12250.
14. He X, Yamada M, Watanabe J, Tiskratok W, Ishibashi M, Kitaura H, *et al.* Titanium nanotopography induces osteocyte lacunar-canalicular networks to strengthen osseointegration. ***Acta Biomater*** 2022;151:613-27.
15. Yamada M, Kato E, Yamamoto A, Sakurai K. A titanium surface with nano-ordered spikes and pores enhances human dermal fibroblastic extracellular matrix production and integration of collagen fibers. ***Biomed Mater*** 2016;11(1):015010.
16. Celles CAS, Teixeira ABV, da Costa Valente ML, Sangali M, Rodrigues JFQ, Caram R, *et al.* Effect of post-processing and variation of the building angle of Ti-6Al-4 V disks obtained by selective laser melting: A comparison of physical, chemical and mechanical properties to machined disks. ***Mater Today Commun*** 2024;39:108700.
17. Lee UL, Yun S, Lee H, Cao HL, Woo SH, Jeong YH, *et al.* Osseointegration of 3D-printed titanium implants with surface and structure modifications. ***Dent Mater*** 2022;38(10):1648-60.
18. Nyberg EL, Farris AL, Hung BP, Dias M, Garcia JR, Dorafshar AH, *et al.* 3D-Printing Technologies for Craniofacial Rehabilitation, Reconstruction, and Regeneration. ***Ann Biomed Eng*** 2017;45(1):45-57.
19. Steinbacher DM. Three-Dimensional Analysis and Surgical Planning in Craniomaxillofacial Surgery. ***J Oral Maxillofac Surg*** 2015;73(12 Suppl):S40-56.
20. Carter LN, Martin C, Withers PJ, Attallah MM. The influence of the laser scan strategy on grain structure and cracking behaviour in SLM powder-bed fabricated nickel superalloy. ***J Alloys Compd*** 2014;615:338-47.
21. Elambasseril J, Rogers J, Wallbrink C, Munk D, Leary M, Qian M. Laser powder bed fusion additive manufacturing (LPBF-AM): the influence of design features and LPBF variables on surface topography and effect on fatigue properties. ***Critical reviews in solid state and materials sciences*** 2023;48(1):132-68.
22. Lin WS, Starr TL, Harris BT, Zandinejad A, Morton D. Additive manufacturing technology (direct metal laser sintering) as a novel approach to fabricate functionally graded titanium implants: preliminary investigation of fabrication parameters. ***Int J Oral Maxillofac Implants*** 2013;28(6):1490-5.
23. Calazans Neto JV, Reis ACD, Valente M. Influence of building direction on physical and mechanical properties of titanium implants: A systematic review. ***Heliyon*** 2024;10(9):e30108.
24. Weissmann V, Drescher P, Seitz H, Hansmann H, Bader R, Seyfarth A, *et al.* Effects of Build Orientation on Surface Morphology and Bone Cell Activity of Additively Manufactured Ti6Al4V Specimens. ***Materials (Basel)*** 2018;11(6):915.
25. Liu W, Li W, Wang H, Bian H, Zhang K. Surface modification of porous titanium and titanium alloy implants manufactured by selective laser melting: A review. ***Advanced Engineering Materials*** 2023;25(21):2300765.
26. Huang LZ, Truong VK, Murdoch BJ, Elbourne A, Caruso RA. Inherent variation in surface roughness of Selective Laser Melting (SLM) printed titanium caused by build angle changes the mechanomicrobiocidal effectiveness of nanostructures. ***Journal of Colloid and Interface Science*** 2025:137866.
27. Luo Y, Jiang Y, Zhu J, Tu J, Jiao S. Surface treatment functionalization of sodium hydroxide onto 3D printed porous Ti6Al4V for improved biological activities and osteogenic potencies. ***J Mater Res Technol*** 2020;9(6):13661-70.
28. Mizutani T, Tsuchiya S, Honda M, Montenegro Raudales JL, Kuroda K, Miyamoto H, *et al.* Alkali-treated titanium dioxide promotes formation of proteoglycan layer and altered calcification and immunotolerance capacity in bone marrow stem cell. ***Biochem Biophys Rep*** 2023;36:101569.
29. Kokubo T, Yamaguchi S. Novel bioactive titanate layers formed on Ti metal and its alloys by chemical treatments. ***Materials*** 2009;3(1):48-63.
30. Lei H, Zhou Z, Liu J, Cao H, Wu L, Song P, *et al.* Structural Optimization of 3D-Printed Porous Titanium Implants Promotes Bone Regeneration for Enhanced Biological Fixation. ***ACS Applied Materials & Interfaces*** 2025;17(12):18059-73.
31. da Costa Valente ML, Uehara LM, Lisboa Batalha R, Bolfarini C, Trevisan RLB, Fernandes RR, *et al.* Current Perspectives on Additive Manufacturing and Titanium Surface Nanotopography in Bone Formation. ***J Biomed Mater Res B Appl Biomater*** 2025;113(3):e35554.
32. Sarker A, Tran N, Rifai A, Brandt M, Tran PA, Leary M, *et al.* Rational design of additively manufactured Ti6Al4V implants to control Staphylococcus aureus biofilm formation. ***Materialia*** 2019;5:100250.
33. Bieler TR, Trevino RM, Zeng L. Alloys: Titanium. In: Bassani F, Liedl GL, Wyder P, editors. Encyclopedia of Condensed Matter Physics. Oxford: Elsevier; 2005. p. 65-76.
34. Arputharaj JD, Nafisi S, Dareh Baghi A, Ghomashchi R. Continuous cooling transformation of L-PBF Ti64. ***J Alloys Comp*** 2025;1021:179700.
35. Wysocki B, Maj P, Sitek R, Buhagiar J, Kurzydłowski KJ, Swieszkowski W. Laser and electron beam additive manufacturing methods of fabricating titanium bone implants. ***Applied Sciences*** 2017;7(7):657.